

Application regime and distortion metric for multivariate RF photonics

A. N. Tait, T. Ferreira de Lima, M. P. Chang, M. A. Nahmias, B. J. Shastri, and P. R. Prucnal

Department of Electrical Engineering, Princeton University, Princeton, NJ, 08544 USA

atait@princeton.edu

Abstract—Photonic weight banks employing multivariate statistical techniques could extend performance limits of multi-antenna radio systems. We characterize the aggregate bandwidth penalty imposed by a silicon microring weight bank and assess application regimes for multivariate RF photonics.

The accelerating demands on spectrum resources are pushing radio operations into new regimes of bandwidth, efficiency, and reconfigurability. A typical radio receiver front-end follows the antenna(s) with analog-to-digital conversion (ADC). ADCs are a bottleneck in RF systems, facing fundamental tradeoffs in sample rate, effective number of bits, and power consumption. Analog RF photonics provide a completely different set of physical processing constraints. Demands for bandwidth, efficiency, and tunability have motivated the development of RF photonics [1]. In an RF photonic front-end, incoming signals are modulated onto an optical carrier and then processed in some way before being detected. ADC occurs after the analog photonic front-end.

As the demand for spectrum access accelerates, the notion of “the spectrum” as a homogeneous entity has begun to erode through the utilization of spatial degrees of freedom (e.g. directionality). Multi-antenna systems introduce a new dimension with which to share radio spectrum based on spatial discrimination. Signals received by phased-array antennas have a high degree of redundancy, so they are typically combined in such a way to distill the most salient information. Central to this is the concept of *dimensionality reduction*, in which information across many channels is fused in an intelligent way to extract a smaller number of information-rich signals. Dimensionality reduction relies on learning the optimal combination of inputs based on statistical analysis. For example, principal component analysis (PCA) is a linear multivariate signal processing task that finds a statistically optimal 1D representation of higher-dimensional data.

To perform these sorts of additions digitally, DSP approaches must perform floating-point multiply-accumulate operations (MACs). Digital receivers for multi-antenna systems present a formidable challenge in that every antenna needs ADC converter, which are performance bottlenecks. With any digital approach, the rate of data to be digitized increases in proportion to the number of antennas. Furthermore, the number of MAC operations required scales with the number of signals. Wideband dimensionality reduction in the analog domain – prior to digitization – would be able to avoid performance tradeoffs between bandwidth, energy use, and

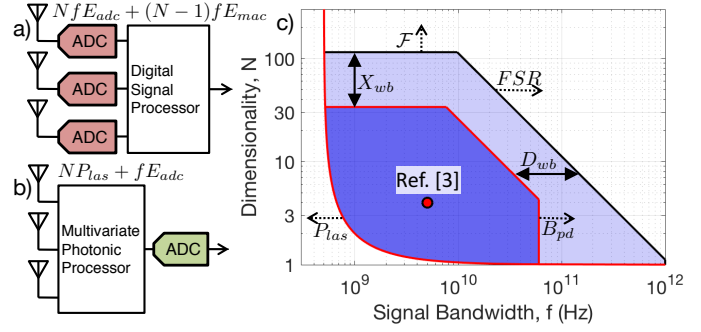


Fig. 1: RF front-ends: a) digital, and b) photonic. c) Application regime of multivariate RF photonics.

number of antennas.

Multivariate RF photonics refers to the application of statistical analysis to photonic implementations of multi-channel RF signal processing. In a multivariate RF photonic receiver, N distinct wavelengths of light carry N signals from N antennas. When WDM signals are detected, the electronic output represents their sum. Using this analog, parallel, and reconfigurable dimensionality reduction, power is not related to bandwidth. An optical technique for converging onto the first principal component of a multi-channel RF signal was developed in [2]. Devices such as wavelength-selective microring (MRR) weight banks allow for this functionality to be integrated on a silicon photonic chip. By tuning filters on and off resonance with their respective signals, an MRR weight bank can individually weight each WDM channel. Prior work on MRR weight banks showed accurate and simultaneous calibration of a bank of 4 MRR weights [3] and a metric to describe the penalty on WDM channel count incurred by weight tuning [4]. Continuing the vein of that work, we here introduce and characterize a metric to describe aggregate bandwidth limits imposed by MRR filter edge dispersion. Furthermore, we perform a preliminary analysis of the regime addressable by multivariate RF photonics, as determined by those metrics.

Regime analysis Microring-based implementations of photonic weight banks have limits imposed by non-ideal filter characteristics. The number of channels that can fit within this range is determined by the ratio of FSR to FWHM, in other words, finesse, \mathcal{F} . We found the penalty on number of channels, N , incurred by weight tunability to be $X_{wb} =$

$\mathcal{F}/N = 3.4$ in [4]. The total aggregate bandwidth, Nf , is limited by FSR, with a penalty of $D_{wb} = Nf/FSR$. In the experiment described below, we found that the maximum signal bandwidth is less than the filter FWHM by a factor of $D_{wb} = 0.23$. Additionally, signal bandwidth is capped by the response of a photonic receiver, B_{pd} , which is up to 60GHz on a silicon photonic platform [5].

Power use is a central criterion for comparing RF front-end performance. For a digital electronic front-end (Fig. 1a), every sample from each of N antennas must be digitized, and then, a minimum of $(N - 1)$ multiply-accumulate (MAC) operations performed. This means $P_{dsp} = NfE_{adc} + (N - 1)fE_{mac}$, where the energy per ADC conversion is $E_{adc} \approx 100\text{pJ}$ [6], and the energy per MAC is $E_{mac} \approx 100\text{pJ}$ [7]. For a photonic front-end (Fig. 1b), a laser is needed for every channel operating at a different wavelength. Because weighting occurs in passive filters and summation occurs through total power detection, no power is consumed in proportion to the operational frequency, besides the single backend ADC. This means $P_{pho} = NP_{las} + fE_{adc}$, where P_{las} is laser wall-plug power. The curve at which $P_{pho} = P_{dsp}$ is plotted in Fig. 1c, putting a lower bound on the regime in which a photonic front-end could be more efficient than a digital front-end. The demonstration of 4-channel, 5GHz MRR weight calibration [3] is plotted for reference.

Aggregate bandwidth penalty In an ideal MRR weight bank, aggregate bandwidth is limited by the resonator free spectral range (FSR). When a MRR is tuned continuously during weighting, the strongly dispersive filter edge distorts high-frequency components of the modulating signal, which introduces a penalty on the usable bandwidth. The maximum signal bandwidth attainable for a given distortion requirement is proportional to the filter bandwidth or full-width half-maximum (FWHM) with a proportionality constant, D_{wb} , for weight bank dispersion. We characterize this distortion experimentally in a fabricated MRR weight bank.

Silicon-on-insulator samples have silicon thickness is 220nm with fully etched waveguides [8]. Ti/Au tuning contacts were then deposited on top of an oxide passivation layer. The sample, mounted on a temperature controlled alignment stage, is coupled to fiber through focusing sub-wavelength grating couplers [9]. The weight bank consists of two bus waveguides and four 10-10.3 μm radius MRRs in a parallel add/drop configuration, each with a thermal tuning element (Fig. 2a). Each MRR has $FSR = 9.0\text{nm}$ and $FWHM = 78\text{pm} = 9.7\text{GHz}$, for a finesse of $\mathcal{F} = 115$. DROP and THRU ports are connected to a balanced photodetector. The weight of a single channel is tuned from weight of -1.0 to $+1.0$ in increments of 0.5, according to the control procedure of Ref. [3]. Simultaneously, an RF complex spectrum analyzer modulating a single laser channel measures the frequency response from 0–15GHz.

Fig. 2b-c shows the RF power transmission from port 1 to port 2 ($|S_{21}|^2$) and the net phase shift, both normalized to the $+1.0$ (off-resonance) weight response. At low frequencies, power transmission depends on absolute weight values of 0,

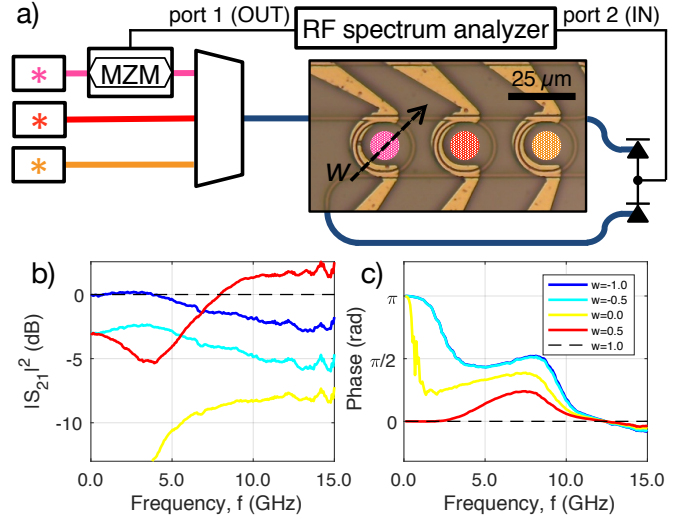


Fig. 2: a) Experimental setup for measuring MRR weight distortion. b) RF power transmission for weight values from -1 to $+1$, normalized to $w = 1$. c) RF phase transmission, showing large distortion of the $w = -1$ trace above 3GHz.

-3 , and $-\infty\text{dB}$, respectively, while the phase is 0 for positive weights and π for negative weights. As frequency increases, power and phase distortion are seen as displacements from constant values. In Fig. 2c, the negatively weighted signals experience a phase distortion of $\pi/2$ at 3.2GHz and $\pi/4$ at 2.2GHz. The allowable distortion depends on system requirements. Supposing a system requirement of $\pi/4$ phase distortion results in $D_{wb} = 0.23$.

Photonic technology could extend the limits of multi-antenna systems into the 10s of GHz and 10s of antennas regime. We have identified factors that place preliminary quantitative bounds on this regime. With continual improvement in resonator quality, laser efficiency, modulator sensitivity, and receiver bandwidths, all driven by the silicon photonic industry, this regime is likely to expand.

REFERENCES

- [1] J. Capmany, J. Mora, I. Gasulla, J. Sancho, J. Lloret, and S. Sales, *Journal of Lightwave Technology*, vol. 31, no. 4, pp. 571–586, Feb 2013.
- [2] A. N. Tait, J. Chang, B. J. Shastri, M. A. Nahmias, and P. R. Prucnal, *Opt. Express*, vol. 23, no. 10, pp. 12 758–12 765, May 2015.
- [3] A. N. Tait, T. Ferreira de Lima, M. A. Nahmias, B. J. Shastri, and P. R. Prucnal, *Opt. Express*, vol. 24, no. 8, pp. 8895–8906, Apr 2016.
- [4] A. N. Tait, A. X. Wu, T. Ferreira de Lima, E. Zhou, B. J. Shastri, M. A. Nahmias, and P. R. Prucnal, *IEEE Journal of Selected Topics in Quantum Electronics*, vol. 22, no. 6, 2016.
- [5] A. Novack, M. Gould, Y. Yang, Z. Xuan, M. Streshinsky, Y. Liu, G. Capellini, A. E.-J. Lim, G.-Q. Lo, T. Baehr-Jones, and M. Hochberg, *Opt. Express*, vol. 21, no. 23, pp. 28 387–28 393, Nov 2013.
- [6] B. Murrmann, *IEEE Solid-State Circuits Magazine*, vol. 7, no. 3, pp. 58–66, Summer 2015.
- [7] B. Marr, B. Degnan, P. Hasler, and D. Anderson, *Very Large Scale Integration (VLSI) Systems, IEEE Transactions on*, vol. 21, no. 1, pp. 147–151, Jan 2013.
- [8] R. J. Bojko, J. Li, L. He, T. Baehr-Jones, M. Hochberg, and Y. Aida, *J. Vac. Sci. Technol., B*, vol. 29, no. 6, 2011.
- [9] Y. Wang, X. Wang, J. Flueckiger, H. Yun, W. Shi, R. Bojko, N. A. Jaeger, and L. Chrostowski, *Opt. Express*, vol. 22, no. 17, pp. 20 652–20 662, 2014.